Suppression of forward dilepton production from an anisotropic quark-gluon plasma

Mauricio Martinez[1,a] and Michael Strickland[2,3]

[1] Helmholtz Research School and Otto Stern School
Goethe - Universität Frankfurt am Main
Ruth-Moufang-Str. 1, 60438 Frankfurt am Main, Germany
[2] Institute für Theoretische Physik and Frankfurt Institute for Advanced Studies
Goethe - Universität Frankfurt am Main
Max-von-Laue-Straße 1, D-60438 Frankfurt am Main, Germany
[3] Department of Physics
Gettysburg College
Gettysburg, PA 17325

Abstract. We calculate the rapidity dependence of leading-order medium dilepton yields resulting from a quark-gluon plasma which has a local time-dependent anisotropy in momentum space. We present a phenomenological model which includes temporal evolution of the plasma anisotropy parameter, ξ, and the hard momentum scale, $p_{\rm hard}$. Our model interpolates between 1+1 dimensional collisionally-broadened expansion at early times and 1+1 dimensional ideal hydrodynamic expansion at late times. Using our model, we find that at LHC energies, forward high-energy medium dilepton production would be suppressed by up to a factor of 3 if one assumes an isotropization/thermalization time of 2 fm/c. Therefore, it may be possible to use forward dilepton yields to experimentally determine the time of onset of locally isotropic hydrodynamic expansion of the quark-gluon plasma as produced in ultrarelativistic heavy-ion collisions.

1 Introduction

Nucleus-nucleus collisions at high energies offer us the opportunity to study experimentally and theoretically a possible new state of matter formed by liberated partons known as a quark-gluon plasma (QGP). Nevertheless, the main goal is not only to discover this new state of matter but also to characterize experimentally many of its properties such as the thermodynamical aspects of this new phase. It is very important to know if the matter created after the collision is really thermalized. In this direction, an open question is to determine the isotropization and thermalization time of the matter, $\tau_{\rm iso}$ and $\tau_{\rm therm}$, respectively.[1] Based on data from the Brookhaven National Lab's Relativistic Heavy Ion Collider (RHIC) early studies found that for $p_T \lesssim 2$ GeV, the elliptic flow, v_2, was very well described by models which assumed ideal hydrodynamic behavior starting at very early times $\tau \sim 0.6$ fm/c [1,2,3]. These fits of v_2 indicated that the matter could be modeled as a nearly-perfect fluid and hence implied fast thermalization of the matter created at RHIC energies. However, recent results from conformal relativistic viscous hydrodynamics [4] have shown that these initial estimates for the isotropization/thermalization time of the plasma are not completely reliable due to poor knowledge of the proper initial

[a] e-mail: guerrero@fias.uni-frankfurt.de

[1] Hereafter, for simplicity, will assume that these two time scales are the same so that $\tau_{\rm therm} = \tau_{\rm iso}$.

conditions (CGC versus Glauber), details of plasma hadronization such as the choice of the proper freezeout time and the subsequent hadronic cascade, etc. Now it seems that isotropization times up to $\tau_{\rm iso} \sim 2$ fm/c are not ruled out by RHIC data. Therefore, additional theoretical and experimental input are necessary to further constrain this time.

One way to increase our understanding of the pre-equilibrium stage of QGP evolution is by studying independent observables which are sensitive to early-time dynamics. One good candidate is high-energy dileptons.[2] Due to their large mean free path, lepton pairs can leave the strongly interacting region carrying information about the earliest times after the nuclear collision. In this work, we calculate the rapidity dependence of dilepton pair production from a QGP which has a time-dependent anisotropy in momentum space.

Most previous phenomenological treatments of dilepton production have assumed that the plasma is thermalized rapidly with $\tau_{\rm iso}$ on the same order as the parton formation time, τ_0. However, due to the rapid 1+1 longitudinal expansion of the plasma at early-times, this assumption seems to be rather strong because it ignores the momentum-space anisotropy developed along the beam axis. Anisotropies in momentum-space are intimately related with Weibel instabilities. Recently, it has been shown that the presence of chromomagnetic Weibel instabilities developed at early times of the collision may affect the value of $\tau_{\rm iso}$ [5,6,7,8,9]. However, it is still not clear how much $\tau_{\rm iso}$ is affected by the presence of these instabilities at phenomenologically accessible collision energies.

Due to the lack of a precise physical picture of the pre-equilibrium QGP, one can instead implement simple models which capture the essence of the complex dynamics at early-times of the collision. This will be our approach in the present work. We propose a simple phenomenological model for the time-dependence of the hard momentum scale, $p_{\rm hard}$, and the plasma anisotropy parameter, $\xi = \langle p_T^2 \rangle / 2 \langle p_L^2 \rangle - 1$. The new aspect in this work compared to our recent proposals for the pre-equilibrium stage of the QGP [10,11,12], is the inclusion of the rapidity dependence of the quark and anti-quark distribution functions. We use fits to experimental data which are available from AGS through RHIC data to constrain the rapidity dependence of the parton distribution functions. Since this rapidity dependence is not perfectly flat we implicitly include effects of the breaking of longitudinal boost invariance of the system.

To make our final phenomenological predictions for dilepton yields, we introduce three different parameters: (1) the parton formation time, τ_0, which is time at which the partons created during the initial hard collision of the nuclei become decoherent and approximately on-shell;[3] (2) $\tau_{\rm iso}$ which is the proper time when the system starts to undergo ideal hydrodynamical expansion; and (3) γ which sets the sharpness of the transition to hydrodynamical behaviour. We assume that for times of the order of τ_0 but smaller than $\tau_{\rm iso}$, the system expands like a collisionally-broadened plasma and smoothly changes to hydrodynamical expansion for times long compared with $\tau_{\rm iso}$. In this work we extend previous calculations [10,11,12] considering the impact of the momentum-space anisotropies on the full rapidity dependence of medium dilepton production. We find that at LHC energies, dilepton yields are suppressed by a factor of 3 around $y \sim 9$ if one chooses $\tau_{\rm iso}$=2 fm/c.

This manuscript is organized as follows: In Sec. 2 we calculate the dilepton production rate at leading order using an anisotropic phase space distribution. In Sec. 3 we present the interpolating model from collisionally-broadened to ideal hydrodynamical expansion including the rapidity dependence of the quark and anti-quark distribution functions. In Sec. 4 we present dilepton yields as a function of the rapidity for different values of $\tau_{\rm iso}$. Finally, we present our conclusions and give an outlook in the Sec. 5.

[2] We mean by high-energy dileptons, lepton pairs with pair transverse momentum (p_T) or invariant mass (M) greater than 1 GeV.

[3] This time can be estimated from the nuclear saturation scale, i.e., $\tau_0 \sim Q_s^{-1}$. For LHC energies, $Q_s \simeq 2$ GeV implying $\tau_0 \simeq 0.1$ fm/c

2 Dilepton rate

From relativistic kinetic theory, the dilepton production rate $dN^{l^+l^-}/d^4Xd^4P \equiv dR^{l^+l^-}/d^4P$ (i.e. the number of dileptons produced per space-time volume and four dimensional momentum-space volume) at leading order in the electromagnetic coupling, α, is given by [14,15,16]:

$$\frac{dR^{l^+l^-}}{d^4P} = \int \frac{d^3\mathbf{p}_1}{(2\pi)^3}\frac{d^3\mathbf{p}_2}{(2\pi)^3} f_q(\mathbf{p}_1) f_{\bar{q}}(\mathbf{p}_2)\, v_{q\bar{q}}\, \sigma^{l^+l^-}_{q\bar{q}}\, \delta^{(4)}(P - p_1 - p_2)\,, \tag{1}$$

where $f_{q,\bar{q}}$ is the phase space distribution function of the medium quarks (anti-quarks), $v_{q\bar{q}}$ is the relative velocity between quark and anti-quark and $\sigma^{l^+l^-}_{q\bar{q}}$ is the total cross section. Since we will be considering high-energy dilepton pairs with center-of-mass energies much greater than the dilepton mass we can ignore the finite dilepton mass corrections and use simply $\sigma^{l^+l^-}_{q\bar{q}} = 4\pi\alpha^2/3M^2$. In addition, we assume that the distribution function of quarks and anti-quarks is the same, $f_{\bar{q}} = f_q$.

Following Ref. [5], we will consider the case that the anisotropic quark/anti-quark phase-space distributions are azimuthally symmetric in momentum space about a direction specified by $\hat{\mathbf{n}}$ and can be obtained from an arbitrary isotropic phase space distribution by squeezing ($\xi > 0$) or stretching ($\xi < 0$) this isotropic distribution function along $\hat{\mathbf{n}}$, i.e.,

$$f_{q,\bar{q}}(\mathbf{p}, \xi, p_{\rm hard}) = f^{iso}_{q,\bar{q}}(\sqrt{\mathbf{p^2} + \xi(\mathbf{p}\cdot\hat{\mathbf{n}})^2}, p_{\rm hard})\,, \tag{2}$$

where $p_{\rm hard}$ is the hard momentum scale, $\hat{\mathbf{n}}$ is the direction of the anisotropy and $\xi > 0$ is a parameter that reflects the strength and type of anisotropy. In the isotropic case, $p_{\rm hard}$ is identified with the temperature of the system and $\xi \equiv 0$. Using the anisotropic distribution given by Eq. (2) into Eq. (1) we obtain:[4]

$$\begin{aligned}\frac{dR^{l^+l^-}}{d^4P} = \frac{5\alpha^2}{18\pi^5}\int_{-1}^{1} d(\cos\theta_{p_1}) \int_{a_+}^{a_-} \frac{dp_1}{\sqrt{\chi}}\, p_1\, f_q\left(\sqrt{\mathbf{p_1^2}(\mathbf{1} + \xi(\tau)\cos^2\theta_{\mathbf{p_1}})}, p_{\rm hard}(\tau,\eta)\right) \\ \times\, f_{\bar{q}}\left(\sqrt{(\mathbf{E} - \mathbf{p_1})^2 + \xi(\tau)(\mathbf{p_1}\cos\theta_{\mathbf{p_1}} - \mathbf{P}\cos\theta_{\mathbf{P}})^2}, p_{\rm hard}(\tau,\eta)\right),\end{aligned} \tag{3}$$

with

$$\begin{aligned}\chi &= 4P^2p_1^2\sin^2\theta_P\sin^2\theta_{p_1} - (2p_1(E - P\cos\theta_P\cos\theta_{p_1}) - M^2)^2\,, \\ a_\pm &= \frac{M^2}{2(E - P\cos(\theta_P \pm \theta_{p_1}))}\,.\end{aligned}$$

For phenomenological predictions of expected dilepton yields, we model the space-time dependence of $p_{\rm hard}$ and ξ. In a realistic non-boost-invariant system $p_{\rm hard}$ will depend of the rapidity on the quark and anti-quark and hence the rate itself will depend not only on the difference of $y - \eta$ but also on η itself. In the next sections we will give details of how this dependence is introduced. Once obtained we can calculate the final rapidity spectra by integrating over phase space:

$$\frac{dN^{l^+l^-}}{dy} = \pi R_T^2 \int dM^2 d^2p_T \int_{\tau_0}^{\tau_f}\int_{-\infty}^{\infty} \frac{dR^{l^+l^-}}{d^4P}\tau d\tau d\eta\,, \tag{4}$$

where $R_T = 1.2\,A^{1/3}$ fm is the radius of the nucleus in the transverse plane. This expression is evaluated in the center-of-mass (CM) frame while the differential dilepton rate is calculated in the local rest frame (LR) of the emitting region. Then, the dilepton pair energy has to be understood as $E_{LR} = p_T\,\cosh(y-\eta)$ in the differential dilepton rate $dR^{l^+l^-}/d^4P$. Substituting

[4] Details of the calculation are presented in Ref. [12].

Eq. (3) into Eq. (4), we obtain the dilepton spectrum as a function of the rapidity including the effect of a time-dependent momentum anisotropy.

One can be worried if either transverse expansion or mixed/hadronic phases in Eq. (4) will affect the production of high-energy dileptons presented here. Fortunately, in the kinematic region studied here this is not the case and these effects turn out to be negligible (1-2% effect) compared with the longitudinal expansion [10].

3 Space Time-Model

In this section, we extend previous models proposed for the pre-equilibrium stage of the QGP [10,11,12] by including a phenomenologically realistic rapidity dependence of the parton distributions. Before presenting the details of the model, we remind the reader of some general relations.

Firstly, the plasma anisotropy parameter is related with the average longitudinal and transverse momentum of the hard particles through the relation:

$$\xi = \frac{\langle p_T^2 \rangle}{2\langle p_L^2 \rangle} - 1 \; . \tag{5}$$

We can obtain two limiting cases from the last expression. For an isotropic plasma, we have that ξ=0, i.e., $\langle p_T^2 \rangle = 2\langle p_L^2 \rangle$. Another possibility is that the partons initially undergo 1d free streaming expansion, where the partons expand freely along the longitudinal axis. Using the free streaming distribution function, it is possible to show that the transverse and longitudinal momentum scales as [9,12,13]:

$$\langle p_T^2 \rangle_{\rm f.s.} \propto 2\, T_0^2 \; , \tag{6a}$$

$$\langle p_L^2 \rangle_{\rm f.s.} \propto T_0^2 \frac{\tau_0^2}{\tau^2} \; . \tag{6b}$$

Inserting these expressions into Eq. (5), one obtains $\xi_{f.s.}(\tau) = \tau^2/\tau_0^2 - 1$. The free streaming result for ξ is the upper-bound on possible momentum-space anisotropies developed during 1d expansion by causality. Modifications to the Eq. (5) result from the different kinds of interactions between the partons, as it is discussed below. In this work, for simplicity, we will not study explicitly the possibility of 1d free streaming expansion since, in reality, this is a rather extreme assumption which requires that the partons do not interact at all. Below we will give details of a more realistic model of the time evolution of the average transverse and longitudinal pressures. However, note that the relation given in Eq. (5) is completely general and can be applied in all cases.

Secondly, for a given anisotropic phase space distribution of the form specified in Eq. (2), the local energy density can be factorized as:

$$\begin{aligned} \mathcal{E}(p_{\rm hard}, \xi) &= \int \frac{d^3\mathbf{p}}{(2\pi)^3}\; p\; f_{\rm iso}(\sqrt{\mathbf{p^2} + \xi(\mathbf{p}\cdot\hat{\mathbf{n}}\mathbf{^2})}, p_{\rm hard}) \; , \\ &= \mathcal{E}_0(p_{\rm hard})\, \mathcal{R}(\xi) \; , \end{aligned} \tag{7}$$

where $\mathcal{E}_0$ is the initial local energy density deposited in the medium at τ_0 and

$$\mathcal{R}(\xi) \equiv \frac{1}{2}\left(\frac{1}{1+\xi} + \frac{\arctan\sqrt{\xi}}{\sqrt{\xi}} \right) . \tag{8}$$

We mention that $p_{\rm hard}$ depends implicitly on proper time and space-time rapidity and that $\lim_{\xi\to 0} \mathcal{R}(\xi) = 1$ and $\lim_{\xi\to\infty} \mathcal{R}(\xi) = 1/\sqrt{\xi}$.

3.1 Momentum-space broadening and plasma instabilities effect

The ratio between the average longitudinal and transverse momentum needed to compute ξ using Eq. (5) is modified from the free streaming case if collisions between the partons are taken into account. To include all relevant $N \leftrightarrow N$ Boltzmann collision terms plus mean field interactions (Vlasov term) is a very difficult task. As a first approximation, one can consider the effect of elastic collisions in the broadening of the longitudinal momentum of the particles. This was the approach in the original version of the bottom-up scenario [13]. In the first stage of this scenario, $1 \ll Q_s\tau \ll \alpha_s^{3/2}$, initial hard gluons have typical momentum of order Q_s and occupation number of order $1/\alpha_s$. Due to the fact that the system is expanding at the speed of light in the longitudinal direction, the density of hard gluons decreases with time, $N_g \sim Q_s^3/(\alpha_s Q_s \tau)$. If there were no interactions this expansion would be equivalent to 1+1 free streaming and the longitudinal momentum p_L would scale like $1/\tau$. However, once elastic $2 \leftrightarrow 2$ collisions of hard gluons are taken into account, the ratio between the longitudinal momentum p_L and the typical transverse momentum of a hard particle p_T decreases as [13]:

$$\frac{\langle p_L^2 \rangle}{\langle p_T^2 \rangle} \propto (Q_s\tau)^{-2/3} \ . \tag{9}$$

Assuming, as before, isotropy at the formation time, $\tau_0 = Q_s^{-1}$, this implies that for a collisionally-broadened expansion, $\xi(\tau) = (\tau/\tau_0)^{2/3} - 1$.

Note that, as obtained in Ref. [13], when collisions are included, it is implicitly assumed that the elastic cross-section is screened at long distances by an isotropic real-valued Debye mass. This is not guaranteed in an anisotropic plasma since the Debye mass can be become complex due to the chromo-Weibel instability. In general, any anisotropic distribution causes the presence of negative eigenvalues in the self-energy of soft gluons [5,6,7,8,9]. Such negative eigenvalues indicate instabilities, which result in exponential growth of chromo-electric and magnetic fields, E^a and B^a, respectively. These fields deflect the particles and how much deflection occurs will depend on the amplitude and domain size of the induced chromofields. Currently, the precise parametric relation between the plasma anisotropy parameter and the amplitude and domain size of the chromofields is not known from first principles.

If one would like to include the momentum-space broadening and the impact of the plasma instabilities, phenomenologically this can be achieved by generalizing the temporal dependence of $\xi(\tau)$ to:

$$\xi(\tau, \delta) = \left(\frac{\tau}{\tau_0}\right)^{\delta} - 1 \ . \tag{10}$$

The exponent δ contains the physical information about the particular type of momentum-space broadening which occurs due to plasma interactions. Two limiting cases for this exponent are the ideal hydrodynamic and free streaming expansion. In the 1+1 hydrodynamical limit, $\delta \equiv 0$ and then $\xi \to 0$. For $\delta \equiv 2$, one recovers the 1+1 dimensional free streaming case, $\xi \to \xi_{\rm f.s.} = (\tau/\tau_0)^2 - 1$. For general δ between these limits one obtains the proper-time dependence of the energy density and temperature by substituting (10) into the general expression for the factorized energy density (7) to obtain $\mathcal{E}(\tau, \delta) = \mathcal{E}_0(p_{\rm hard})\, \mathcal{R}(\xi(\tau, \delta))$. The inclusion of the rapidity dependence of the parton distribution functions is discussed in Sec. 3.2.

Different values of δ arise dynamically from the different processes contributing to parton isotropization. For example, elastic collisional-broadening results in Eq. (9) and hence $\delta = 2/3$. Recently, some authors have considered the values of δ resulting from processes associated with the chromo-Weibel instability presented at the earliest times after the initial nuclear impact [17,18,19]:

$$\frac{\langle p_L^2 \rangle}{\langle p_T^2 \rangle} \sim (Q_s\tau)^{-\frac{1}{2}\left(\frac{1}{1+\nu}\right)} \ , \tag{11}$$

where

$$\nu = \begin{cases} 0 \ \text{Ref.[17]} & , \\ 1 \ \text{Ref.[18]} & , \\ 2 \ \text{Nielsen-Olesen limit, Ref.[19]} \ . \end{cases} \tag{12}$$

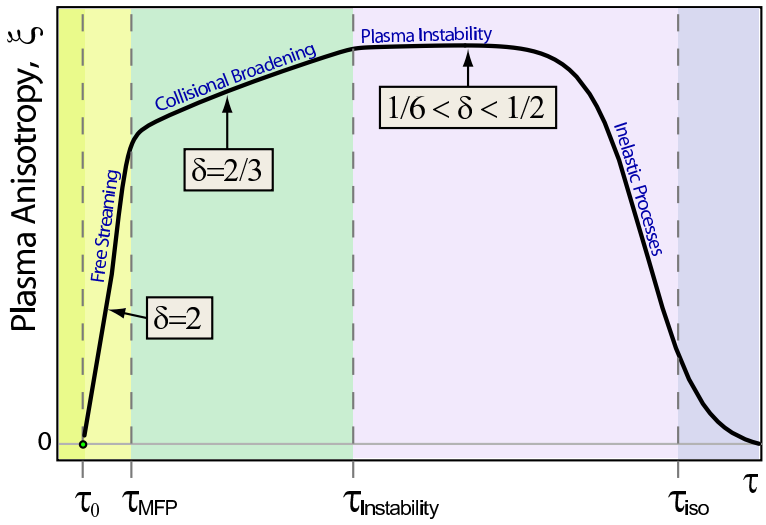

Fig. 1. Sketch of the time dependence the plasma anisotropy indicating the various time scales and processes taking place. Here $\tau_{\rm MFP}$ is the mean time between elastic collisions (mean-free time) and $\tau_{\rm Instability}$ is the time at which plasma-instability induced soft modes have grown large enough to affect hard particle dynamics.

Summarizing, the coefficient δ in Eq. (10) takes on the following values

$$\delta = \begin{cases} 2 & \text{Free streaming expansion ,} \\ 2/3 & \text{Collisional-Broadening, Ref.[13] ,} \\ 1/2 & \text{Ref.[17] ,} \\ 1/4 & \text{Ref.[18] ,} \\ 1/6 & \text{Nielsen-Olesen limit, Ref.[19] ,} \\ 0 & \text{Hydrodynamic expansion .} \end{cases} \tag{13}$$

In Fig. 1 we sketch the time-dependence of the plasma anisotropy parameter indicating the time scales at which the various processes become important. At times shorter than the mean time between successive elastic scatterings, $\tau_{\rm MFP}$, the system will undergo 1+1 dimensional free streaming with $\delta = 2$. For times long compared to $\tau_{\rm MFP}$ but short compared to $\tau_{\rm Instability}$ the plasma anisotropy will grow with the collisionally-broadened exponent of $\delta = 2/3$. Here $\tau_{\rm Instability}$ is the time at which instability-induced soft gauge fields begin to influence the hard-particles' motion. When $\tau_{\rm Instability} < \tau < \tau_{\rm iso}$ the plasma anisotropy grows with the slower exponent of $\delta = 1/6 \ldots 1/2$ due to the bending of particle trajectories in the induced soft-field background. At times large compared to $\tau_{\rm Instability}$ inelastic processes are expected to drive the system back to isotropy [13]. We note here that for small ξ and realistic couplings it has been shown [20] that one cannot ignore the effect of collisional-broadening of the distribution functions and that this may completely eliminate unstable modes from the spectrum.

Based on such a sketch, one could try to construct a detailed model which includes all of the various time scales and study the dependence of the process under consideration on each. However, there are theoretical uncertainties in each of these time scales and their dependences on experimental conditions. We choose to use a simpler approach in which we will construct a phenomenological model which smoothly interpolates the coefficient δ from the 1d collisionally-broadened expansion to 1d hydrodynamical expansion, i.e., $2/3 \geq \delta \geq 0$.

In the model we introduce a transition width, γ^{-1}, which governs the smoothness of the transition from the initial value of $\delta = 2/3$ to $\delta = 0$ at $\tau \sim \tau_{\rm iso}$. The collisionally-broadened interpolating model provides us a realistic estimate of the effect of plasma anisotropies. Note that by using such a smooth interpolation one can achieve a reasonable phenomenological description of the transition from non-equilibrium to equilibrium dynamics which should hopefully

capture the essence of the physics. In the next section we will give mathematical definitions for the model.

3.2 Interpolating model for collisionally broadened expansion

In order to construct an interpolating model between collisionally-broadened and hydrodynamical expansion, we introduce the smeared step function:

$$\lambda(\tau, \tau_{\rm iso}, \gamma) \equiv \frac{1}{2}\left(\tanh\left[\frac{\gamma(\tau-\tau_{\rm iso})}{\tau_{\rm iso}}\right]+1\right) \ , \tag{14}$$

where γ^{-1} sets the width of the transition between non-equilibrium and hydrodynamical evolution in units of $\tau_{\rm iso}$. In the limit when $\tau \ll \tau_{\rm iso}$, we have $\lambda \to 0$ and when $\tau \gg \tau_{\rm iso}$ we have $\lambda \to 1$. Physically, the energy density $\mathcal{E}$ should be continuous as we change from the initial non-equilibrium value of δ to the final isotropic $\delta = 0$ value appropriate for ideal hydrodynamic expansion. Once the energy density is specified, this gives us the time dependence of the hard momentum scale. We find that for general δ this can be accomplished with the following model:

$$\xi(\tau,\delta) = (\tau/\tau_0)^{\delta(1-\lambda(\tau))} - 1 \ , \tag{15a}$$

$$\mathcal{E}(\tau,\eta) = \mathcal{E}_0 \ \mathcal{R}\left(\xi\right) \ \bar{\mathcal{U}}^{4/3}(\tau) \ F^4(\eta) \ , \tag{15b}$$

$$p_{\rm hard}(\tau,\eta) = T_0 \ \bar{\mathcal{U}}^{1/3}(\tau) \ F(\eta) \ , \tag{15c}$$

with $\mathcal{R}(\xi)$ defined in Eq. (8) and for fixed final multiplicity we have:

$$\mathcal{U}(\tau) \equiv \left[\mathcal{R}\Big(\left(\tau_{\rm iso}/\tau_0\right)^{\delta}-1\Big)\right]^{3\lambda(\tau)/4} \left(\frac{\tau_{\rm iso}}{\tau}\right)^{1-\delta(1-\lambda(\tau))/2} \ ,$$

$$\bar{\mathcal{U}}(\tau) \equiv \mathcal{U}(\tau)\,/\,\mathcal{U}(\tau^+_{\rm iso}) \ , \tag{16a}$$

$$\mathcal{U}(\tau^+_{\rm iso}) \equiv \lim_{\tau\to\tau^+_{\rm iso}} \mathcal{U}(\tau) = \left[\mathcal{R}\Big(\left(\tau_{\rm iso}/\tau_0\right)^{\delta}-1\Big)\right]^{3/4} \left(\frac{\tau_{\rm iso}}{\tau_0}\right) \ . \tag{16b}$$

and $\delta = 2/3$ for the case of 1d collisionally broadened expansion interpolating to 1d ideal hydrodynamic expansion.

Recently, models for the pre-equilibrium stage in the presence of momentum-space anisotropies have been applied in the central rapidity region of high-energy dileptons [10,11,12]. Here we extend these previous analyses through the inclusion of rapidity dependence of the parton hard momentum scale by using a phenomenologically constrained "rapidity profile function," $F(\eta)$. Our main goal with this modification is to explore the phenomenological consequences in the forward rapidity region where the effect of early-time anisotropies are expected to be maximal. We are not attempting to describe the physics of the forward rapidity region from first principles,[5] instead, we implement a Gaussian fit profile for the rapidity dependence which successfully describes experimentally observed pion rapidity spectra from AGS to RHIC energies [25,26,27,28,29] and use this to extrapolate to LHC energies:

$$F(\eta) = \exp\left(-\frac{\eta^2}{2\sigma_\eta^2}\right) \ , \tag{17}$$

with

$$\sigma_\eta^2 = \frac{8}{3}\frac{c_s^2}{(1-c_s^4)}\ln\left(\sqrt{s_{NN}}/2m_p\right) \ , \tag{18}$$

where c_s is the sound velocity and m_p is the proton mass.

[5] Some proposals have been mentioned in the literature, see Ref. [21,22,23,24]

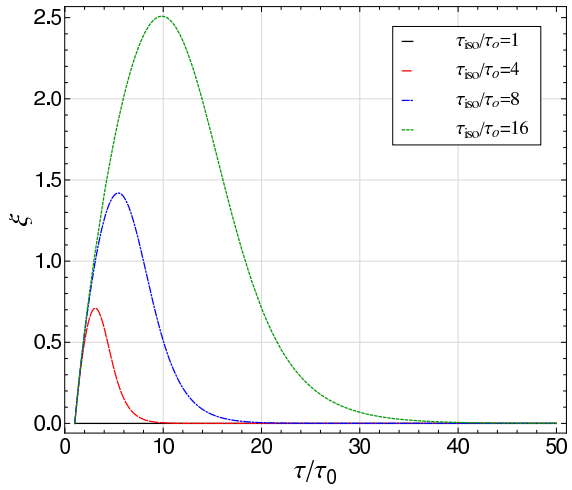

Fig. 2. Temporal evolution of the plasma anisotropy parameter using our collisionally-broadened interpolating model for four different isotropization times $\tau_{\rm iso} \in \{1, 4, 6, 18\}\,\tau_0$. The transition width is taken to be $\gamma = 2$. To convert to physical scales use $\tau_0 \sim 0.1$ fm/c for LHC energies.

Note that once the rapidity dependence in the parton momentum distribution functions is implemented boost invariance along the longitudinal axis breaks down. This procedure leads to a violation of the conservation laws expressed by hydrodynamics unless a finite baryon chemical potential is introduced [30]. It is possible to demonstrate that for a longitudinal scaling expansion, $\partial\mathcal{P}(T,\mu)/\partial\eta$=0, where $\mathcal{P}$ is the pressure and T is the temperature. This condition is equivalent to:[6]

$$s\frac{\partial T}{\partial \eta} + n\frac{\partial \mu}{\partial \eta} = 0\,, \tag{19}$$

where s and n denote the entropy density and particle number density, respectively. In the present context don't have to worry about the presence of finite chemical potentials since we are considering high-energy dilepton production and $E/T \gg \mu/T$ is satisfied. Therefore, in the differential dilepton rate dR/d^4P, Eq.(1), the product of the distribution functions $f_q(\mathbf{p}_q, +\mu)\; f_{\bar{q}}(\mathbf{p}_{\bar{q}}, -\mu) \approx f_q(\mathbf{p}_q)\; f_{\bar{q}}(\mathbf{p}_{\bar{q}})$.

In Fig. 2, the temporal evolution of the anisotropy parameter $\xi(\tau)$ is plotted using Eq. (15a). In Fig. 3, we show the time and rapidity dependence of $p_{\rm hard}(\tau,\eta)$ (right and left panel, respectively) using Eq. (15c).

4 Results

In this section, we will present our predicted dilepton yields as a function of the rapidity from a Pb-Pb collision at LHC full beam energy, $\sqrt{s_{NN}}$= 5.5 TeV. At this center-of-mass energy we use τ_0= 0.088 fm/c, T_0= 845 MeV, R_T= 7.1 fm and the critical temperature T_c=160 MeV. The kinematic cuts in the transverse momentum and invariant mass of the dilepton yields are indicated in the corresponding results. Also, we use $c_s^2 = 1/3$ and $m_p = 0.938$ GeV in Eq. (18).

Before presenting our results we first explain the numerical procedure used for our calculations. Because the differential dilepton rate $dR^{l^+l^-}/d^4P$ given in Eq. (3) is independent of the assumed space-time model, we first evaluate it numerically using double-exponential integration with a target precision of 10^{-9}. The result for the rate was then tabulated on a uniformly-spaced 4-dimensional grid in M, p_T, y, and ξ: $M/p_{\rm hard}, p_T/p_{\rm hard} \in \{0.1, 20\}$, $y \in \{-10, 10\}$ and

[6] Partial derivatives with respect to η are performed at constant τ.

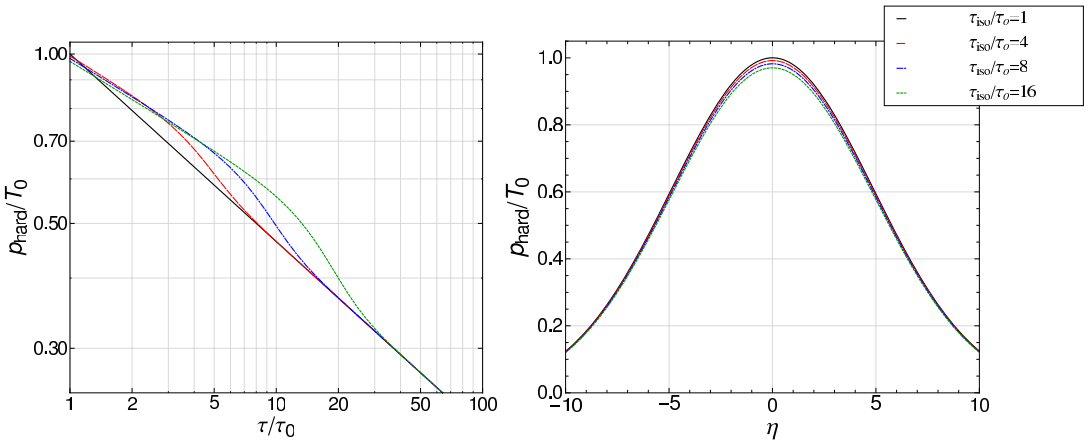

Fig. 3. Temporal evolution (left panel) and rapidity dependence (right panel) of the hard momentum scale, $p_{\rm hard}$ using our fixed final multiplicity collisionally-broadened interpolating model for the hard momentum scale for four different isotropization times $\tau_{\rm iso} \in \{1, 4, 8, 16\}\,\tau_0$. The transition width is taken to be $\gamma = 2$. To convert to physical units use $\tau_0 \sim 0.1$ fm/c for LHC energies. For the rapidity dependence of $p_{\rm hard}$ (right panel) we used a constant value of $\tau \sim 0.1$ fm/c and the width $\sigma_\eta^2 \sim 8$.

$\xi \in \{0, 5\}$. This table was then used to build a four-dimensional interpolating function which was valid at continuous values of these four variables. We then boost this rate from the local reference frame to center-of-mass frame and evaluate the remaining integrations over space-time (τ and η), transverse momentum and invariant mass appearing in Eq. (4) using quasi-Monte Carlo integration with $\tau \in \{\tau_0, \tau_f\}$, $\eta \in \{-10, 10\}$ and, depending on the case, restrict the integration to any cuts specified in M or p_T.

Our final integration time, τ_f, is set by solving numerically for the point in time at which the temperature in our interpolating model is equal to the critical temperature, i.e. $p_{\rm hard}(\tau_f, \eta) = T_C$. We will assume that when the system reaches T_C, all medium emission stops. Note that due to the fact that $p_{\rm hard}$ depends on the parton rapidity, the plasma lifetime now depends on which rapidity slice you are in, with higher rapidities having a shorter lifetime due to their lower initial "temperature". We are not taking into account the emission from the mixed/hadronic phase at late times since the kinematic regime we study (high M and p_T) is dominated by early-time high-energy dilepton emission [10,16].

We show our predicted dilepton spectrum as a function of the pair rapidity, y, for LHC energies using our model described by Eqs. (15) in Fig. 4. From this, we see that for LHC energies there is a suppression when we vary the isotropization time from τ_0 to 2 fm/c. This suppression can be explained qualitatively by two mechanisms. The first one, the anisotropic nature of the distribution function as a consequence of the rapid expansion implies that dileptons with larger values of longitudinal momentum are reduced compared with the case of an isotropic distribution function. The suppression will depend on the maximum amount of momentum-space anisotropy achieved at early times and also on the time dependence of the anisotropy parameter ξ; in this work, we consider a realistic scenario for a collisionally-broadened plasma. The other source of rapidity dependence of the final dilepton spectra is related to the fact that the hard momentum scale ("temperature") depends explicitly on the rapidity η, even in the case of instantaneous thermalization. To generate Fig. 4 we have applied a cut $M \geq 2$ GeV and $P_T \geq 100$ MeV. As can be seen from this figure a isotropization time of $\tau_{\rm iso} = 2$ fm/c results in fewer dileptons as compared to "instantaneous" isotropization $\tau_{\rm iso} = 0.088$ fm/c. This suppression is enhanced at forward rapidities.

In order to quantify the effect of the pre-equilibrium emission we define the "dilepton modification" factor as the ratio of the dilepton yield obtained with an isotropization time of $\tau_{\rm iso}$ to that obtained from an instantaneously thermalized plasma undergoing only 1+1 hydrody-

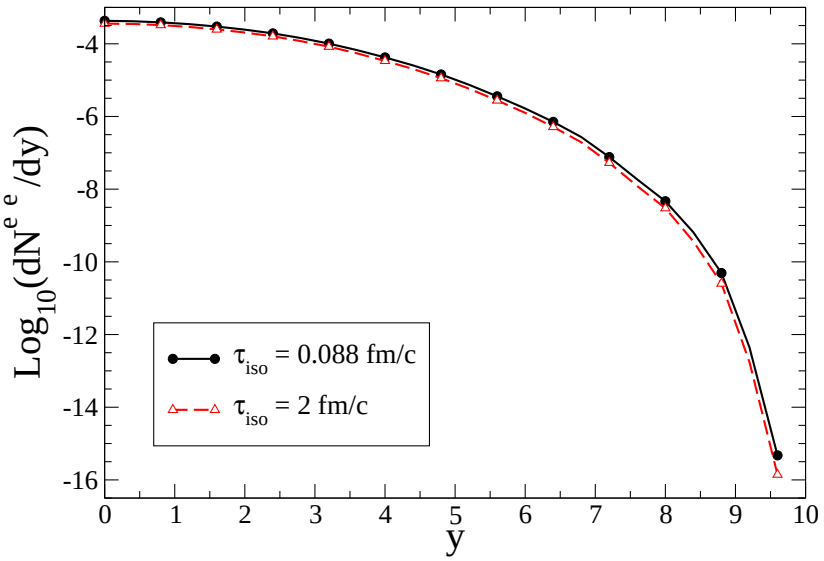

Fig. 4. Fixed final multiplicity condition collisionally-broadened interpolating model dilepton yields as a function of rapidity in Pb-Pb collisions at LHC, with a cut $M \geq 2$ GeV and $P_T \geq 100$ MeV. For medium dileptons we use $\gamma = 2$ and $\tau_{\rm iso}$ to be either 0.088 or 2 fm/c for LHC energies.

namical expansion, ie. $\tau_{\rm iso} = \tau_0$:

$$\Phi(\tau_{\rm iso}) \equiv \left(\frac{dN^{e^+e^-}(\tau_{\rm iso})}{dy} \right) \Bigg/ \left(\frac{dN^{e^+e^-}(\tau_{\rm iso} = \tau_0)}{dy} \right) . \tag{20}$$

This ratio measures how large the effect of early-time momentum anisotropies are on medium dilepton production. In the case of instantaneous isotropization, $\Phi(\tau_{\rm iso})$ is unity, and for $\tau_{\rm iso} > \tau_0$ any deviation from unity indicates a modification of medium dilepton production due to pre-equilibrium emissions.

In Fig. 5 we show our prediction for the rapidity dependence of the high-energy dilepton modification factor, $\Phi(\tau_{\rm iso})$, for three different assumed plasma isotropization times, $\tau_{\rm iso} \in \{$ 0.1,1,2$\}$ fm/c. To generate this figure we have applied a cut $M \geq 2$ GeV and $P_T \geq 100$ MeV. As can be seen from this figure a isotropization time of $\tau_{\rm iso} = 2$ fm/c results in fewer dileptons as compared to "instantaneous" isotropization $\tau_{\rm iso} = 0.088$ fm/c. This suppression is enhanced at forward rapidities and reaches a maximum suppression of a factor of 3 at extremely forward rapidities.

Using the dilepton modification factor as our criterion we find that for our collisionally-broadened interpolating model with fixed final multiplicity, the dilepton yields as a function of the rapidity at $\tau_{iso} = 2$ fm/c can be suppressed up to $\sim 20\%$ for $0 < y \lesssim 4$. The suppression of dilepton yields is more dramatic at rapidity values around $y \sim 9$ and can be as large as a factor of 3. With sufficiently accurate experimental results this could give an experimental method for determining the isotropization time of a quark gluon plasma as formed in an ultrarelativistic nuclear collision.

5 Conclusions

In this work we have introduced a phenomenological model that takes into account early-time momentum-space anisotropies in the rapidity dependence of high-energy dilepton production. To do this we have modeled the temporal evolution of the plasma anisotropy parameter ξ and the hard momentum scale $p_{\rm hard}$. To study the dilepton production rapidity dependence, we

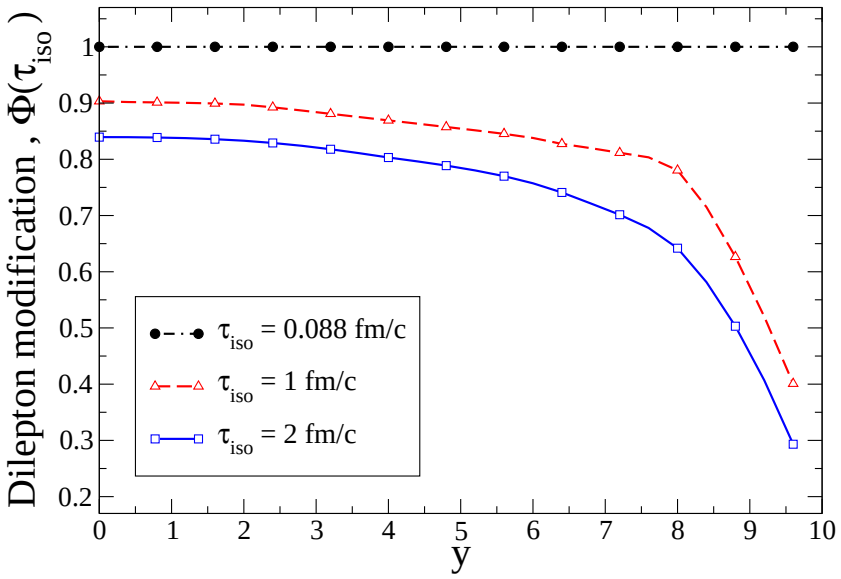

Fig. 5. Predicted dilepton modification factor, $\Phi(\tau_{\rm iso})$, for three different assumed plasma isotropization times, $\tau_{\rm iso} \in \{$ 0.1,1,2$\}$ fm/c. Cuts are the same as in Fig. 4.

have parametrized the rapidity dependence of $p_{\rm hard}$ using a Gaussian profile which is consistent with experimental observations of final pion spectra from AGS through RHIC energies.

We have applied the proposed model to study high-energy dilepton yields as a function of the pair rapidity and find that this observable is sensitive to the chosen value of $\tau_{\rm iso}$. This suppression can be explained as a consequence of the combined effect of the anisotropy in momentum-space achieved at early-times due to expansion and the rapidity dependence of the hard momentum scale which explicitly breaks longitudinal boost invariance. We find that with the resulting dilepton modification factor, $\Phi(\tau_{\rm iso}$=2 fm/c), shows suppressed dilepton yields in the forward rapidity region which can be up to 20% for $0 < y \lesssim 4$ and up to a factor of 3 at $y \sim 9$. The amplitude of the suppression of $\Phi(\tau_{\rm iso})$ could help us to experimentally constrain $\tau_{\rm iso}$ given sufficiently precise data in the forthcoming LHC experiments. In this way forward dileptons would provide a way to determine the plasma isotropization time experimentally.

An uncertainty of our treatment comes from our implicit assumption of chemical equilibrium. If the system is not in chemical equilibrium (too many gluons and/or too few quarks) early time quark chemical potentials, or fugacities, will affect the production of lepton pairs [15,16]. However, to leading order, the quark and gluon fugacities will cancel between numerator and denominator in the dilepton suppression factor, $\Phi(\tau_{\rm iso})$ [16]. We, therefore, expect that to good approximation one can factorize the effects of momentum space anisotropies and chemical non-equilibrium.

We note in closing that the interpolating model presented here can be applied to other observables than dilepton yields. Indeed, with this model it is possible to assess the phenomenological consequences of momentum-space anisotropies on other observables which are sensitive to early-time stages of the QGP, e.g. photon production, heavy-quark transport, jet-medium induced electromagnetic and gluonic radiation, etc.

Acknowledgments

We thank A. Dumitru, S. Jeon, M. Bleicher, H. Appelshäuser and B. Schenke for helpful discussions. M. Martinez thanks N. Armesto and C. Salgado for assistance provided in order to attend the Hard Probes 2008 conference where this work was initiated. M. Martinez was

supported by the Helmholtz Research School and Otto Stern School of the Goethe-Universität Frankfurt am Main. M.S. was supported by DFG project GR 1536/6-1. M.S. also acknowledges support from the Yukawa Institute for Theoretical Physics during the "Entropy Production Before QGP" workshop.

References

1. P. Huovinen, P. F. Kolb, U. W. Heinz, P. V. Ruuskanen and S. A. Voloshin, Phys. Lett. B **503** (2001).
2. T. Hirano and K. Tsuda, Phys. Rev. C **66** (2002) 054905.
3. M. J. Tannenbaum, Rept. Prog. Phys. **69** (2006) 2005.
4. M. Luzum and P. Romatschke, arXiv:0804.4015 [nucl-th].
5. P. Romatschke and M. Strickland, Phys. Rev. D **68** (2003) 036004.
6. S. Mrowczynski and M. H. Thoma, Phys. Rev. D **62** (2000) 036011.
7. P. Arnold, J. Lenaghan and G. D. Moore, JHEP **0308** (2003) 002.
8. P. Romatschke and M. Strickland, Phys. Rev. D **70**, 116006 (2004).
9. A. Rebhan, M. Strickland and M. Attems, Phys. Rev. D 78, 045023 (2008).
10. M. Martinez and M. Strickland, Phys. Rev. Lett. **100**, (2008) 102301.
11. M. Martinez and M. Strickland, arXiv:0804.2618 [hep-ph].
12. M. Martinez and M. Strickland, arXiv:0805.4552 [hep-ph].
13. R. Baier, A. H. Mueller, D. Schiff and D. T. Son, Phys. Lett. B **502** (2001) 51.
14. J.I. Kapusta, L.D. McLerran and D.Srivastava, Phys. Lett. B **283**, (1992) 145.
15. A. Dumitru, D.H. Rischke, T. Schonfeld, L. Winckelmann, H. Stoecker and W. Greiner, Phys. Rev. Lett. **70**, (1993) 2860.
16. M. Strickland, Phys. Lett. B **331**, 245 (1994).
17. D. Bodeker, JHEP **0510** (2005) 092.
18. P. Arnold and G. D. Moore, Phys. Rev. D **73** (2006) 025013.
19. P. Arnold and G. D. Moore, Phys. Rev. D **76** (2007) 045009.
20. B. Schenke, M. Strickland, C. Greiner and M. H. Thoma, Phys. Rev. D **73** (2006) 125004.
21. T. Renk, Phys. Rev. C **70** (2004) 021903.
22. T. Hirano and Y. Nara, Nucl. Phys. A **743** (2004) 305.
23. T. Hirano, Phys. Rev. C **65** (2002) 011901.
24. K. Morita, S. Muroya, C. Nonaka and T. Hirano, Phys. Rev. C **66** (2002) 054904.
25. I. G. Bearden *et al.* [BRAHMS Collaboration], Phys. Rev. Lett. **94** (2005) 162301.
26. I. C. Park *et al.* [PHOBOS Collaboration], Nucl. Phys. A **698** (2002) 564.
27. B. B. Back *et al.* [PHOBOS Collaboration], Phys. Rev. C **74** (2006) 021901.
28. G. I. Veres *et al.* [PHOBOS Collaboration], arXiv:0806.2803 [nucl-ex].
29. M. Bleicher, arXiv:hep-ph/0509314.
30. A. Dumitru, U. Katscher, J. A. Maruhn, H. Stoecker, W. Greiner and D. H. Rischke, Z. Phys. A **353** (1995) 187.